Physical and biogeochemical modulation of ocean acidification in the central North Pacific

John E. Dore[a,1], Roger Lukas[b], Daniel W. Sadler[b], Matthew J. Church[b], and David M. Karl[b,1]

[a]Department of Land Resources and Environmental Sciences, Montana State University, Bozeman, MT 59717; and [b]Department of Oceanography, University of Hawaii, Honolulu, HI 96822

Contributed by David M. Karl, June 8, 2009 (sent for review April 10, 2009)

Atmospheric carbon dioxide (CO_2) is increasing at an accelerating rate, primarily due to fossil fuel combustion and land use change. A substantial fraction of anthropogenic CO_2 emissions is absorbed by the oceans, resulting in a reduction of seawater pH. Continued acidification may over time have profound effects on marine biota and biogeochemical cycles. Although the physical and chemical basis for ocean acidification is well understood, there exist few field data of sufficient duration, resolution, and accuracy to document the acidification rate and to elucidate the factors governing its variability. Here we report the results of nearly 20 years of time-series measurements of seawater pH and associated parameters at Station ALOHA in the central North Pacific Ocean near Hawaii. We document a significant long-term decreasing trend of -0.0019 ± 0.0002 y^{-1} in surface pH, which is indistinguishable from the rate of acidification expected from equilibration with the atmosphere. Superimposed upon this trend is a strong seasonal pH cycle driven by temperature, mixing, and net photosynthetic CO_2 assimilation. We also observe substantial interannual variability in surface pH, influenced by climate-induced fluctuations in upper ocean stability. Below the mixed layer, we find that the change in acidification is enhanced within distinct subsurface strata. These zones are influenced by remote water mass formation and intrusion, biological carbon remineralization, or both. We suggest that physical and biogeochemical processes alter the acidification rate with depth and time and must therefore be given due consideration when designing and interpreting ocean pH monitoring efforts and predictive models.

carbon cycle | climate change | CO_2 | pH | Station ALOHA

When gaseous CO_2 is dissolved in seawater, it reacts to form carbonic acid (H_2CO_3), which undergoes a series of reversible dissociation reactions that release hydrogen (H^+) ions:

$$CO_2 + H_2O \rightleftharpoons H_2CO_3 \rightleftharpoons H^+ + HCO_3^- \rightleftharpoons 2H^+ + CO_3^{2-} \quad [1]$$

The concentration of H^+ (in mol kg^{-1} seawater) approximates its activity and determines the acidity of the solution. Acidity is commonly expressed on a logarithmic scale as pH:

$$pH = -\log_{10}[H^+] \quad [2]$$

The addition of CO_2 therefore acidifies seawater and lowers its pH. Over the past 250 years, the mean pH of the surface global ocean has decreased from ≈8.2 to 8.1, which is roughly equivalent to a 30% increase in $[H^+]$ (1–3). This acidification of the sea is driven by the rapidly increasing atmospheric CO_2 concentration, which results from fossil fuel combustion, deforestation, and other human activities. Models predict that surface ocean pH may decline by an additional 0.3–0.4 during the 21st century (3, 4); over time, turbulent mixing, subduction, and advection are expected to transport anthropogenic CO_2 from the seasonally mixed layer into the ocean interior, lowering the pH of these deeper waters as well (4). Crucial marine biogeochemical processes may be altered, and many marine organisms may be negatively impacted by such pH reductions (2, 3, 5). As ocean CO_2 accumulates, seawater becomes more corrosive to calcium carbonate ($CaCO_3$); hence, those organisms that use structural components made of $CaCO_3$ are especially at risk (2, 3). Direct effects of elevated aqueous CO_2 on metabolic processes and indirect effects due to pH-dependent changes in chemical speciation are also predicted consequences of continued acidification (1, 2, 5). Accurate assessments of the rate of ocean acidification, and improvements in our understanding of the factors regulating its progress, are therefore of considerable importance.

There are 4 measurable parameters of the carbonic acid system in seawater: pH, dissolved inorganic carbon (DIC), total alkalinity (TA), and CO_2 partial pressure (pCO_2). Any pair of these can be used to describe the entire system; however, such calculations rely on empirically derived apparent dissociation "constants," which are themselves functions of temperature and salinity [see *SI Text* regarding these calculations]. In addition, because seawater nutrients are biologically altered in a nonconservative manner, minor contributions of phosphate and silicate to TA must be considered. Often, DIC and TA are determined along with salinity, temperature, phosphate, and silicate, and used to calculate pCO_2, pH, and the concentrations of the various aqueous carbonic acid species. The surface ocean pCO_2 (pCO_{2oce}) is also commonly measured, along with atmospheric pCO_2 (pCO_{2atm}); the flux of CO_2 across the air-sea interface depends on their difference and on the wind speed (6).

Measurements of seawater pH are less often obtained than those of DIC, TA, or pCO_{2oce} despite the facility and precision of the colorimetric analytical method (7). Direct pH measurements are made soon after collection on sealed samples held at a fixed temperature (typically 25 °C) and are usually reported on the total hydrogen ion scale ($^{25tot}pH_{meas}$). The total scale is used for analytical and operational convenience when dealing with seawater media; it differs from the free scale, in that hydrogen ions found in ionic association with sulfate are considered along with truly free hydrogen ions (7). Corresponding pH values at in situ temperature and pressure ($^{istot}pH_{meas}$) are derived from these fixed-temperature measurements using empirical relationships. Seawater pH may also be calculated from DIC and TA at in situ conditions ($^{istot}pH_{calc}$) or, for comparative purposes, at the same fixed temperature used for the direct pH measurements ($^{25tot}pH_{calc}$); fixed-temperature pH provides information on processes influencing DIC and TA, free from the effects of temperature variations on H_2CO_3 equilibria.

Author contributions: J.E.D., R.L., and D.M.K. designed research; J.E.D., D.W.S., and M.J.C. performed research; J.E.D., R.L., D.W.S., M.J.C., and D.M.K. analyzed data; and J.E.D. wrote the paper.

The authors declare no conflict of interest.

Freely available online through the PNAS open access option.

See Commentary on page 12213.

[1]To whom correspondence should be addressed at: Department of Land Resources and Environmental Sciences, Montana State University, 334 Leon Johnson Hall, Bozeman, MT 59717. E-mail: jdore@montana.edu and dkarl@hawaii.edu.

This article contains supporting information online at www.pnas.org/cgi/content/full/0906044106/DCSupplemental.

Despite the urgency of the ocean acidification problem, there are few available data sets directly documenting its long-term (decadal to interdecadal) rate or its shorter-term (seasonal to interannual) variability. Repeat hydrography has been used to document a decadal increase in the inventory of DIC in the Pacific (8); however, the technique has not yet been applied to the detection of pH changes. Long-term trends in pCO_{2oce} globally have also been documented from large data synthesis efforts (9), but these results do not directly address pH and are confined to the surface layer. Although such approaches provide important spatial coverage of long-term trends, their accuracy will be difficult to assess unless seasonal and interannual time scales of pH variability can be adequately resolved. Long time-series pH records from specific locations offer a powerful means to assess both trends and such time scales of variability in ocean acidification. Time-series pH records have recently been reported for the surface layers of 3 open-ocean sites (2, 10–12) and for a coastal tide pool (13). Surface pH at the open-ocean sites (BATS and ESTOC in the western and eastern subtropical North Atlantic, respectively, and ALOHA in the subtropical North Pacific) revealed similar long-term decreasing trends that were generally consistent with equilibration of the surface ocean with rising atmospheric CO_2 (2, 10–12). The 8-year record from Tatoosh Island on the North American west coast revealed a more rapid pH decline, but this data set is complicated by very strong seasonal and even daily variability several times greater than corresponding pH variability at the open ocean sites (13). Although the factors driving seasonal and interannual variability in surface DIC, TA, and pCO_{2oce} at the oceanic time-series stations have been the foci of numerous reports (11, 12, 14–18), less attention has been given to surface pH variability at these sites (12), and their subsurface pH has not yet been discussed.

Since October 1988, the Hawaii Ocean Time-series (HOT) program has measured a suite of physical and biogeochemical properties at Station ALOHA (22.75 °N, 158 °W) in the North Pacific subtropical gyre, at nearly monthly intervals. Here, we present data on seawater pH and related parameters from the initiation of the time-series through 2007. We refine and update earlier estimates of the long-term surface (0–30 m) pH trend, examine pH trends in the subsurface waters and how they vary with depth, and analyze the seasonal and interannual variability in surface layer pH and its possible causes. We also compare pH values derived from DIC and TA with direct pH measurements and discuss the causes and consequences of slight differences between the 2 data sets.

Results

Long-Term Trends in Seawater pH. At Station ALOHA, pCO_{2oce} was well below pCO_{2atm} most of the time (see Fig. 1). The ocean was therefore a net sink for atmospheric CO_2 at this site during each year of observation (17). Although pCO_{2atm} and especially pCO_{2oce} exhibited seasonal and interannual variability, their overall 19+-year trends (mean ± SE) were statistically indistinguishable: +1.68 ± 0.03 and + 1.88 ± 0.16 μatm y^{-1}, respectively. The long-term rise in pCO_{2oce} was mirrored by a decline in surface ocean $^{istot}pH_{calc}$ (see Fig. 1); the observed rate of pH decline (−0.0019 ± 0.0002 y^{-1}) compared well with the rate predicted based on equilibration of atmospheric CO_2 with the surface seawater (−0.0016 ± 0.00003 y^{-1}; see Table S1). Although based on fewer data, the trend in surface layer $^{istot}pH_{meas}$ (-0.0014 ± 0.0002 y^{-1}) was only slightly less negative than, and statistically indistinguishable from, the trend in $^{istot}pH_{calc}$ (see Fig. 1 and Table S1).

DIC at Station ALOHA increases with depth to a maximum near 800–1000 m, roughly coincident with a pronounced oxygen minimum layer (see Fig. 2), reflecting the impact of decades of organic matter mineralization within this water mass and the influence of low-oxygen waters from beneath highly productive areas near the North American west coast (19). TA also increases with depth, but its distribution more closely follows salinity, with a local maximum near 200 m and a pronounced minimum near 400–500 m, slightly above the salinity minimum at 550 m. The anomalous data points evident between 300–400 m result from the passage of a low-oxygen, high-salinity eddy during January 2001 (20); these points were not used in any of our calculations. From the DIC, TA, and salinity data, along with corresponding measurements of silicate and phosphate, we calculated $^{25tot}pH_{calc}$ and $^{istot}pH_{calc}$ throughout the 4,730-m water column from October 1988 to December 2007. The $^{istot}pH_{calc}$ profile decreased from surface values ≈8.1 to minimum values near 7.6 in the low-oxygen, high-DIC intermediate waters (see Fig. 2). We also performed full water column measurements of $^{25tot}pH_{meas}$ from April 1992 to June 1998 and again from June 2003 to December 2007, and from these data derived $^{istot}pH_{meas}$ (see Fig. 2). Overall, the consistency of the measured and calculated pH values was excellent: the mean difference ($^{25tot}pH_{calc}$ minus $^{25tot}pH_{meas}$) of 1964 direct comparisons was 0.0032, and the root mean square of these differences was 0.0120.

In situ pH trends were observed from the surface to at least 600 m (see Fig. 2). Above 300 m, these trends were statistically significant at the 95% confidence level. However, the acidification rates did not decrease monotonically with depth. Subsurface maxima in the acidification rate were observed at 250 m and 400–500 m. Differences were also apparent (although not significant) between the in situ pH trends and those determined at

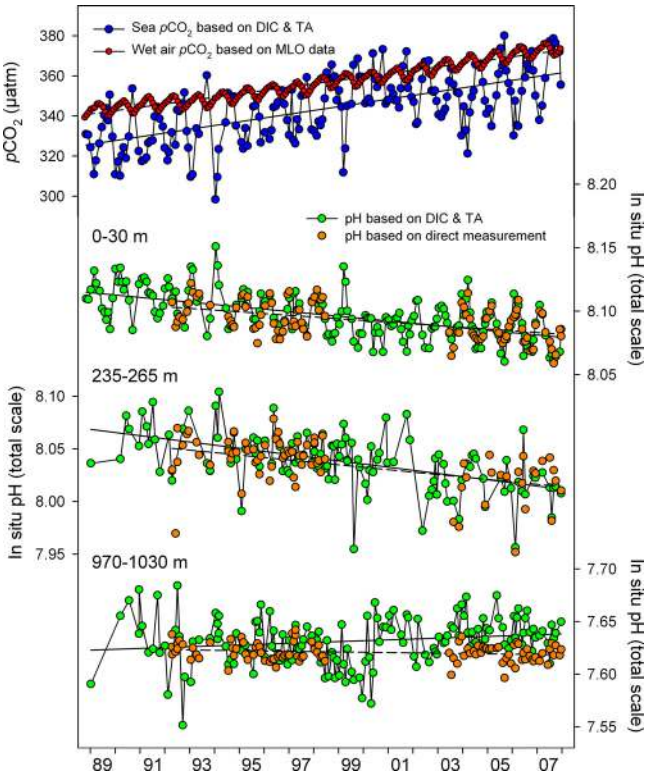

Fig. 1. Time-series of mean carbonic acid system measurements within selected depth layers at Station ALOHA, 1988–2007. (First image) Partial pressure of CO_2 in seawater calculated from DIC and TA (blue symbols) and in water-saturated air at in situ seawater temperature (red symbols). Linear regressions of the sea and air pCO_2 values are represented by solid and dashed lines, respectively. (Second, third, and fourth images) In situ pH, based on direct measurements (orange symbols) or as calculated from DIC and TA (green symbols), in the surface layer and within layers centered at 250 and 1000 m. Linear regressions of the calculated and measured pH values are represented by solid and dashed lines, respectively.

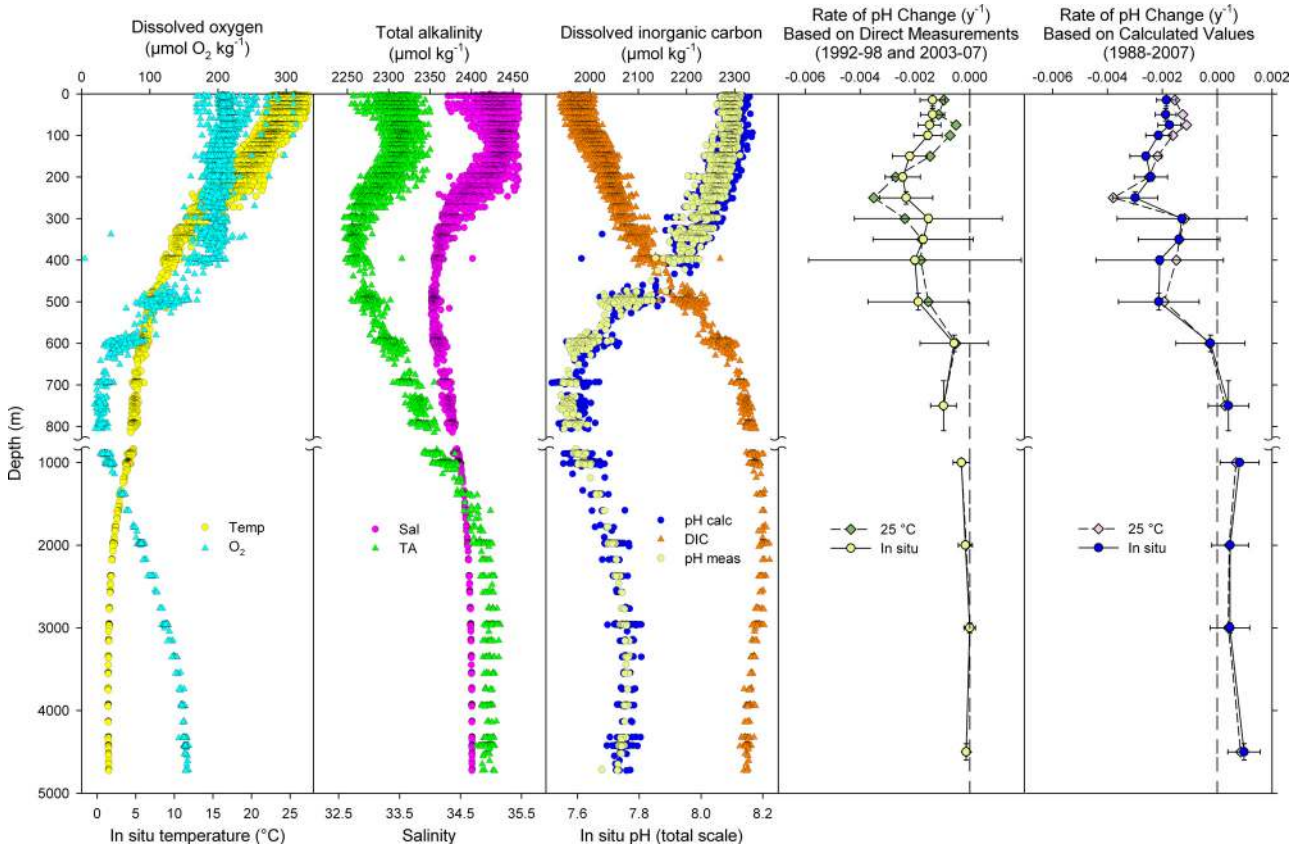

Fig. 2. Depth distributions of carbonic acid system measurements, key physical parameters and seawater pH trends within selected depth ranges at Station ALOHA, 1988–2007. (First, second, and third images) In situ temperature, dissolved oxygen, salinity, total alkalinity, dissolved inorganic carbon, and in situ pH based on direct measurements and as calculated from DIC and TA. (Fourth and fifth images) Long-term trends in seawater pH based on direct measurements and as calculated from DIC and TA. Direct pH measurements were made only from 1992–1998 and 2003–2007. Symbols represent the slopes of linear regressions of pH with time of all data within each depth interval as indicated by vertical error bars. Horizontal error bars represent the 95% confidence intervals of the regression slopes. Trends were separately calculated for in situ conditions (circles) and at a fixed temperature of 25 °C at atmospheric pressure (diamonds). For clarity, error bars are shown only for in situ values; the depth intervals for corresponding trends at 25 °C are identical and the confidence intervals are nearly so.

fixed temperature. Within the upper 150 m, the rate of acidification in situ exceeded the rate at 25 °C; the peak acidification rate, at 250 m, was slightly greater at 25 °C than it was in situ (see Fig. 2). Additionally, there were differences between the pH trends based on measured values and those based on values calculated from DIC and TA. From the surface down to 600 m, the agreement between the corresponding directly measured and calculated results was good. However, the trends based on $^{istot}pH_{calc}$ and $^{25tot}pH_{calc}$ indicated small increases in pH over time in the deeper waters; those based on $^{istot}pH_{meas}$ and $^{25tot}pH_{meas}$ displayed a gradual diminishment in magnitude with depth but never turned positive (see Fig. 2).

Seasonal and Interannual Variability in Surface Layer pH. Superimposed on the long-term declining trend of the surface layer pH at Station ALOHA was a robust seasonal oscillation (see Fig. 1). To better characterize this seasonality, we removed the long-term linear trends from the surface layer $^{istot}pH_{calc}$ and $^{25tot}pH_{calc}$ data sets and binned the detrended observations by calendar month; we then compared the monthly mean detrended pH values to those of mixed layer depth and surface layer temperature (see Fig. 3). In situ pH displayed a winter (January to April) maximum and a summer (July to October) minimum, in a mirror image of the temperature pattern. At a fixed temperature, pH displayed a distinctly different seasonality; minimum $^{25tot}pH_{calc}$ corresponded more closely with minimum temperature, and vice versa. The annual period of decreasing $^{25tot}pH_{calc}$ (November to February) corresponded with the deepest mixed layers, and the period of increasing $^{25tot}pH_{calc}$ (May to August) corresponded with the shallowest mixed layers (see Fig. 3).

To examine interannual pH variability, we first determined $^{25tot}pH_{calc}$ using a constant salinity of 35 and values of DIC, TA, phosphate, and silicate that were adjusted by the ratio 35/salinity (e.g., nDIC = 35DIC/salinity and nTA = 35TA/salinity). By using this salinity normalization procedure, the effects of interannual changes in the surface evaporation/precipitation balance (17) were removed from the pH data; by calculating pH at 25 °C, the effects of temperature changes on pH were similarly removed. We then removed both the long-term trend and the remaining seasonal cycle from the salinity-normalized surface layer $^{25tot}pH_{calc}$ data set and compared its detrended temporal pattern with that of the similarly detrended and filtered mixed layer depth data set (see Fig. 4). Because surface nTA at ALOHA is essentially constant (-0.06 ± 0.06 μmol kg^{-1} y^{-1}), the remaining pH anomaly captures variability caused mainly by interannual changes in the DIC balance of the surface ocean, independent of temperature and salinity variations, average seasonal cycles, and the relentless progress of atmospheric CO_2 invasion. The pH anomaly record revealed fairly small anomalies from 1989–1997, then an abrupt transition to strongly negative anomalies during 1998. From 2000–2003, the pH anomaly steadily rose, and then it became strongly positive and remained

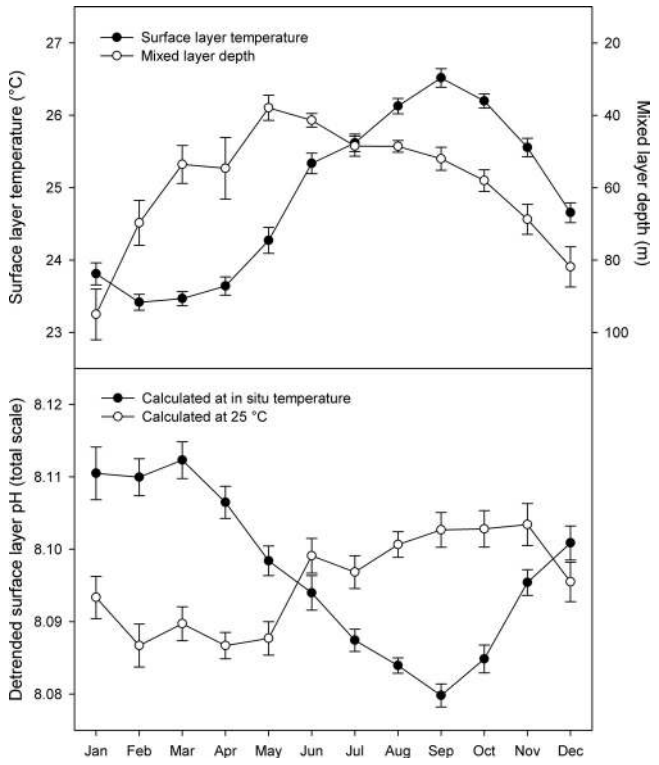

Fig. 3. Seasonal cycles of surface layer physical parameters and pH at Station ALOHA, 1988–2007. (*Upper*) Monthly mean surface layer (0–30 m) temperature (solid symbols) and mixed layer depth (open symbols). (*Lower*) Monthly mean detrended surface layer in situ pH calculated from DIC and TA (solid symbols) or at 25 °C (open symbols). Vertical error bars represent ± 1 standard error. The number of observations for each monthly value ranges from 13 to 20.

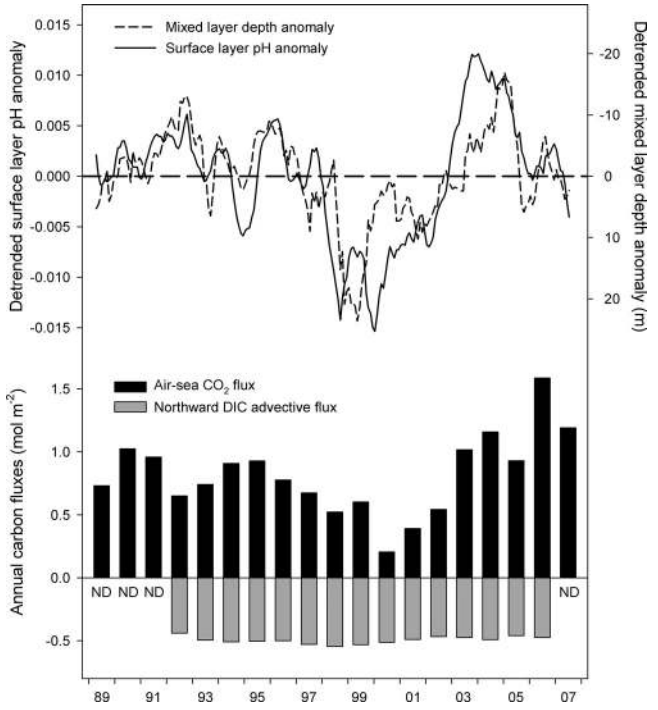

Fig. 4. Interannual variability in surface ocean pH, mixed layer depth and key inorganic carbon fluxes at Station ALOHA, 1989–2007. (*Upper*) Anomalies of fixed-temperature, constant salinity pH (calculated from DIC and TA at 25 °C and salinity = 35; solid curve) and mixed layer depth (dashed curve). Anomalies are defined as positive when pH values are higher than normal or mixed layers are deeper than normal. (*Lower*) Annual flux of atmospheric CO_2 into the surface ocean (black bars) and estimated annual northward export of DIC from the surface ocean via horizontal advection (gray bars). ND, no advective flux data for this year.

so through 2004. During 2005, the pH anomaly returned to near zero values and remained there through 2007. The mixed layer depth anomaly followed a reversed pattern; the 11-month running means of the 2 anomalies were anticorrelated ($r = -0.71$) with no time lag (see Fig. 4). Anomalously low surface pH was thus correlated with unusually deep mixing, which entrains high-DIC, low-pH waters from below the surface layer (see Fig. 1). Annual advective fluxes of DIC from Station ALOHA, which were estimated from modeled current velocities and a measured DIC gradient for the region (see *SI Text*), were relatively constant over the period of observation (see Fig. 4). Air-sea CO_2 fluxes, while variable, did not appear to exert an influence on surface pH variability. For example, low fluxes of CO_2 into the sea from 1998–2002 corresponded with low pH and relatively high fluxes during 2003–2005 were coincident with high pH (see Fig. 4); the opposite pattern would be expected if variability in the atmospheric CO_2 invasion was the primary driver of anomalous DIC accumulation.

Discussion

Depth Variability of Long-Term pH Trends. The rate of surface pH decline at Station ALOHA (see Fig. 1) is similar to those observed at the BATS and ESTOC time-series stations (10–12). A precise comparison is complicated by differences in the time periods of measurement and in the types of pH data used in the trend determinations. A trend of -0.0017 ± 0.0001 y^{-1} from September 1983 to December 2005 was reported for $^{istot}pH_{calc}$ using the combined records from BATS and nearby Hydrostation S (11). At ESTOC, a trend for $^{25tot}pH_{meas}$ of -0.0017 ± 0.0004 y^{-1} from October 1995 to February 2004 was reported (12). At ALOHA, the respective trends (y^{-1}) in $^{istot}pH_{calc}$ and $^{25tot}pH_{meas}$ were -0.0019 ± 0.0002 (October 1988 to December 2007) and -0.0009 ± 0.0002 (April 1992 to December 2007) (see Fig. 2 and Table S1). The difference between the measured and calculated surface pH trends at ALOHA is largely due to the gaps in the measured pH data set. A slightly slower decline of pH at 25 °C relative to that of pH at in situ conditions (see Fig. 2) can be attributed to a mixed layer temperature trend of $+0.026 \pm 0.016$ °C y^{-1} observed over the period of study; due to temperature effects on carbonic acid dissociation constants, pH decreases with increasing temperature by approximately -0.015 °C^{-1} for given values of DIC and TA.

Beneath the surface layer, the long-term pH trends show considerable variability with depth. The most rapid pH decline in situ is found at 250 m (see Fig. 2). The acidification rate of these interior waters appears slightly faster when considered at a fixed temperature. Over the period of observation, the waters in this layer have undergone a significant freshening that is partially density-compensated by a significant cooling trend (21, 22). These changes are indicative of changes in the relative rates of evaporation and precipitation at 28–35 °N, where the associated water mass forms. Subduction and transport of this water along a constant potential density horizon brings it to Station ALOHA in a layer between 160–310 m about 5 years later (21, 22). The temperature trend in this layer of approximately -0.008 °C y^{-1} should result in a physical contribution to the in situ pH trend of $+0.0002$ y^{-1}, which is roughly consistent with the difference between the observed in situ and fixed temperature pH trends (see Fig. 2).

The elevated acidification rate at 250 m is not accompanied by an nTA trend, therefore it is primarily attributable to the more rapid accumulation of nDIC within this layer (1.86 ± 0.30 μmol

$kg^{-1}\ y^{-1}$) compared to that within the surface layer (0.85 ± 0.08 μmol $kg^{-1}\ y^{-1}$). This accelerated increase of nDIC may be a result of a temporal increase in surface DIC at the formation area for the water mass, or it could be related to changes in the formation location and therefore in the chemical characteristics of the source waters. Once these waters are isolated from the atmosphere, biological remineralization of organic carbon at depth may continue to impact their DIC content in a nonconservative manner during their transit to ALOHA. Organic carbon export from the euphotic zone, via gravitational settling of particles and by downward turbulent mixing of dissolved compounds, has varied considerably over our study period (16, 18, 23). About 60% of this passively exported carbon is converted back to DIC through microbiological respiration between 150–300 m, and another 20% is remineralized between 300–500 m (23, 24). An additional contribution to carbon remineralization within the 300–500 m layer is made by the metabolism of vertically migrating mesozooplankton (25, 26). These organisms actively transport organic carbon consumed in the surface waters at night to these depths and there respire it during the day, releasing CO_2. Significant increases in both the primary photosynthetic production of organic carbon and the total mesozooplankton biomass have been documented at Station ALOHA since about 1997, associated with climate-induced changes to the stability of the upper ocean (25–27). An increase in respiration of exported organic carbon by microheterotrophs may therefore contribute to the acidification peak at 250 m, and enhanced mesozooplankton respiration may contribute to acidification in the 400–500 m layer. However, we have to date found no significant long-term decreases in oxygen concentration within these subsurface layers, such as would be expected to accompany nDIC accumulation via enhanced biological respiration (5). Any such evidence of a biological contribution to the enhanced subsurface acidification rates is likely masked by larger physical mixing and transport effects on DIC and oxygen.

The HOT program focuses its sampling on the upper 200 m; less intensive sampling contributes to the relatively large error bars on the acidification rates within some deeper layers, particularly those centered at 300 and 400 m (see Fig. 2). Despite these uncertainties, the estimated rates remain nonzero to at least 600 m and perhaps as deep as 1,000 m, consistent with the estimated penetration depth of anthropogenic CO_2 into the water column (28). In the deep ocean, acidification is not measureable on our 19-year time scale, although confidence in the regressions is better due to the near constancy of pH. However, the errors in pH trends at great depth based on calculated pH values are considerably larger than those based on direct pH measurements (see Fig. 1), and the former display positive values while the latter yield near-zero values (see Fig. 2). These differences underscore the need for caution when using DIC and TA to calculate pH for estimating deep ocean trends. Such calculations amplify errors associated with the individual measurements, and these amplified errors have the potential to impact the estimated pH trends, particularly if they occur near the beginning or end of the time-series. Because of the age of intermediate and deep waters at ALOHA, accumulation of DIC has driven them far from equilibrium with atmospheric CO_2 (see Fig. 1), thus there is greater potential for DIC (and pH) to change during sample processing, storage, and analysis than is encountered with near-surface samples. In addition, samples for DIC and TA are stored in borosilicate glass bottles before analysis on shore; leaching of silicate (29) and borate into the samples over time has the potential to raise their alkalinity, hence changes to glass composition or storage conditions could alter calculated pH. Importantly, seawater CO_2 reference materials (30), which are certified for DIC and TA but not for pH, have never been prepared with waters as acidic as those found below ≈400 m at Station ALOHA; the $^{25tot}pH_{calc}$ of each batch prepared to date has been ≥7.8. Samples for direct colorimetric pH measurements are collected in stoppered quartz cuvettes and analyzed within a few hours; hence, such measurements are less likely to be subject to potential storage artifacts. Also, the absolute accuracy of the direct pH measurements is a function of the inherent chemical properties of the *m*-cresol purple indicator dye, not on calibration of standards (7). For these reasons, we recommend that colorimetric measurements of pH be used along with measurements of DIC and TA in efforts to monitor the progress of ocean acidification.

Temporal Variability of Surface pH. Daily heating and cooling, along with photosynthesis and respiration, result in a diurnal pH cycle (13). HOT program sampling is not designed to characterize such high-frequency variability, but we have observed daily changes of as much as 0.01 in surface pH. To minimize potential biases in seasonal and longer-term analyses due to such daily rhythms, sampling for CO_2 system parameters is conducted at night except when prevented due to unforeseen changes in ship operations. In all, 90% of the surface layer samples used here were collected between 17:00 and 05:00 Hawaii Standard Time and 82% were collected between 19:00 and 01:00. Therefore, we are confident that the observed seasonal and interannual patterns and long-term trends are not influenced by changes in the time of day of sampling.

Seasonal variations in pH have the potential to either accelerate or slow the progress of ocean acidification (31). At Station ALOHA, surface pH exhibits a distinct seasonality in situ that is driven mainly by the seasonal temperature cycle and its impact on carbonic acid equilibria (see Fig. 3). When pH is determined at a fixed temperature, a different pattern emerges. With the effect of temperature changes removed, pH remains low during the period of relatively deep winter mixing and high during summer stratification (see Fig. 3). This pattern is driven by the entrainment of DIC-rich waters from below during winter and the biological drawdown of this DIC during summer (15–17). One needs to make the distinction between the in situ and 25 °C pH cycles, especially when comparing different sites. For example, published surface pH data from BATS (11) and ESTOC (12) appear to exhibit quite different seasonal patterns, but the difference is primarily due to the latter results being reported at 25 °C and the former at in situ temperature. Although the pH measurements are made at a fixed temperature, it is the in situ pH that directly influences the chemistry and biology of the oceans.

The observed interannual variability in surface pH (see Fig. 4) is related mainly to factors governing the relative input and output fluxes of DIC. Air-sea exchange, mixing, and entrainment, horizontal transport, and biological drawdown and export all contribute to the net DIC balance (15, 16, 18). We see in Fig. 4 that interannual variability of air-sea exchange and horizontal transport do not appear to be important factors governing the interannual patterns in surface pH at ALOHA. Interannual variations in the DIC balance are thus primarily affected by the relative strengths of DIC input via turbulent mixing and the biological DIC drawdown and export (i.e., net community production) (16). Relatively deep mixing enhances the upward flux of DIC into the surface layer, directly lowering surface pH; the lack of temporal offset between the pH and mixed layer depth anomalies (see Fig. 4) is consistent with this mechanism. During periods of prolonged stratification, anomalously low quantities of DIC are brought upward, thus the pH drifts higher. Beyond this direct, DIC-related effect on pH, photosynthetic DIC assimilation may be stimulated following periods of strong mixing due to the entrainment of growth-limiting nutrients, especially nitrate (NO_3^-) (27). However, at ALOHA, the molar DIC:NO_3^- of the entrained waters is higher than the canonical 106:16 "Redfield" C:N ratio associated with nutrient-sufficient

phytoplankton growth (32). Hence, NO_3^- stimulation of net community production cannot remove all of the excess DIC brought up by enhanced mixing.

There is a non-Redfield growth scenario under which more DIC may be exported via net community production than is entrained by mixing. An excess of phosphate (PO_4^{3-}) over NO_3^-, relative to the 16:1 Redfield N:P, exists in the subsurface waters at Station ALOHA (32, 33). If this excess P, combined with high light due to stratification, sufficiently stimulates nitrogen (N_2) fixation by photosynthetic cyanobacteria in the surface layer, N limitation of net community production may be alleviated and there can be a net biological sequestration of DIC (15, 32, 33). It has recently been suggested that deliberate fertilization of the surface ocean with PO_4^{3-} at sites like Station ALOHA might enhance the net removal of atmospheric CO_2 to the deep sea via this mechanism (32). We suspect that the period of rapid pH increase at ALOHA (1999–2003), which followed a period of anomalously deep mixing (1997–1999), was at least partially driven by a naturally occurring version of this P-fertilization process (see Fig. 4). If stimulation of net community production by NO_3^- had proceeded at Redfield C:N:P, without extra N delivery via N_2 fixation, DIC should have accumulated and pH should not have risen to anomalously high levels. Importantly, not only the pH anomaly but the in situ pH itself rose during the 5-year period following enhanced mixing (see Fig. 1). Although this unprecedented reversal of ocean acidification was temporary, and the ultimate fate of the carbon fixed has not been definitively ascertained, such an anomalous event underscores the need to better understand the physical and biological controls on ocean pH and their feedback mechanisms. Moreover, this prolonged reversal of surface layer acidification highlights the utility of long-term, full water column pH monitoring; had HOT started collecting surface samples alone in 1999, we may have concluded after 5 years that Station ALOHA's waters were becoming less acidic with time.

Materials and Methods

Shipboard sampling was conducted in all but a few cases within 10 km of the nominal location of Station ALOHA. A rosette sampling package was used to collect discrete 12-L bottle samples at up to 24 depths per hydrographic cast. The package was outfitted with a SeaBird CTD sensor system for vertical profiling of salinity (conductivity), temperature, depth (pressure), and dissolved oxygen. Subsamples were preserved for subsequent laboratory analyses of salinity, DIC, TA, phosphate, silicate, and dissolved oxygen. Sensor calibrations, sampling protocols, and analytical procedures followed standard HOT methods (see *SI Text*). Calculated values of pH and pCO_{2oce} were obtained from these measured parameters using independently validated parameterizations of the apparent dissociation constants for H_2CO_3 in seawater. Direct measurements of pH were made at sea using the colorimetric *m*-cresol purple method (7). Details regarding the CO_2 system calculations, the data sets used and the statistical analyses used in this study may be found in *SI* (see *SI Text*).

ACKNOWLEDGMENTS. Time-series research inevitably builds on the pioneering contributions of numerous individuals; we thank all of the past and present scientists, staff, students, ships' crews, and support personnel who have helped to generate the HOT data set. We also thank C. Winn, D. Hebel, C. Carrillo, P. Driscoll, L. Tupas, and C. Sabine for their efforts to establish and maintain the quality and continuity of the HOT CO_2 system measurements; L. Fujieki and F. Santiago-Mandujano for time-series data management; A. Dickson, P. Quay, and the late C. Keeling for their collaboration; and P. Brewer and R. Wanninkhof for thoughtful reviews of an earlier version of this paper. Meteorological data sets and current velocity estimates were obtained from the National Oceanic and Atmospheric Administration (NOAA) and the Massachusetts Institute of Technology, respectively. This research was funded by the National Science Foundation, the NOAA, the Department of Energy, the State of Hawaii, and the Gordon and Betty Moore Foundation.

1. Raven J, *et al.* (2005) *Ocean Acidification Due to Increasing Atmospheric Carbon Dioxide*. (The Royal Society, London).
2. Doney SC, Fabry VJ, Feely RA, Kleypas JA (2009) Ocean acidification: The other CO_2 problem. *Annu Rev Marine Sci* 1:169–192.
3. Orr JC, *et al.* (2005) Anthropogenic ocean acidification over the twenty-first century and its impact on calcifying organisms. *Nature* 437:681–686.
4. Caldeira K, Wickett ME (2005) Ocean model predictions of chemistry changes from carbon dioxide emissions to the atmosphere and ocean. *J Geophys Res* 10.1029/2004JC002671.
5. Brewer PG, Peltzer ET (2009) Limits to marine life. *Science* 324:347–348.
6. Wanninkhof R (1992) Relationship between wind speed and gas exchange over the ocean. *J Geophys Res* 97:7373–7382.
7. Clayton TD, Byrne RH (1993) Spectrophotometric seawater pH measurements: Total hydrogen ion concentration scale calibration of *m*-cresol purple and at-sea results. *Deep-Sea Res I* 40:2115–2129.
8. Sabine CL, *et al.* (2008) Decadal changes in Pacific carbon. *J Geophys Res* 10.1029/2007JC004577.
9. Takahashi T, *et al.* (2009) Climatological mean and decadal change in surface ocean pCO_2, and net sea-air CO_2 flux over the global oceans. *Deep-Sea Res II* 56:554–577.
10. Bindoff NL et al. (2007) in *Climate Change 2007*: *The Physical Science Basis. Contribution of Working Group I to the Fourth Assessment Report of the Intergovernmental Panel on Climate Change*, eds Solomon S, et al. (Cambridge University Press, Cambridge).
11. Bates NR (2007) Interannual variability of the oceanic CO_2 sink in the subtropical gyre of the North Atlantic Ocean over the last 2 decades. *J Geophys Res* 10.1029/2006JC003759.
12. Santana-Casiano JM, González-Dávila M, Rueda M-J, Llinás O, González-Dávila E-F (2007) The interannual variability of oceanic CO_2 parameters in the northeast Atlantic subtropical gyre at the ESTOC site. *Global Biogeochem Cycles* 10.1029/2006GB002788.
13. Wootton JT, Pfister CA, Forester JD (2008) Dynamic patterns and ecological impacts of declining ocean pH in a high-resolution multi-year dataset. *Proc Natl Acad Sci USA* 105:18848–18853.
14. Winn CD, Li Y-H, Mackenzie FT, Karl DM (1998) Rising surface ocean dissolved inorganic carbon at the Hawaii Ocean Time-series site. *Mar Chem* 60:33–47.
15. Bates NR, Michaels AF, Knap AH (1996) Seasonal and interannual variability of oceanic carbon dioxide species at the U.S. JGOFS Bermuda Atlantic Time-series study (BATS) site. *Deep-Sea Res II* 43:347–383.
16. Quay P, Stutsman J (2003) Surface layer carbon budget for the subtropical N. Pacific: $\delta^{13}C$ constraints at Station ALOHA. *Deep-Sea Res I* 50:1045–1061.
17. Dore JE, Lukas R, Sadler DW, Karl DM (2003) Climate-driven changes to the atmospheric CO_2 sink in the subtropical North Pacific Ocean. *Nature* 424:754–757.
18. Keeling CD, Brix H, Gruber N (2004) Seasonal and long-term dynamics of the upper ocean carbon cycle at Station ALOHA near Hawaii. *Global Biogeochem Cycles* 10.1029/2004GB002227.
19. Wyrtki K (1962) The oxygen minima in relation to ocean circulation. *Deep-Sea Res* 9:11–23.
20. Lukas R, Santiago-Mandujano F (2001) Extreme water mass anomaly observed in the Hawaii Ocean Time-series. *Geophys Res Lett* 28:2931–2934.
21. Lukas R, Santiago-Mandujano F (2008) Interannual to interdecadal salinity variations observed near Hawaii: Local and remote forcing by surface freshwater fluxes. *Oceanography* 21:46–55.
22. Stammer D, Park S, Köhl A, Lukas R, Santiago-Mandujano F (2008) Causes for large-scale hydrographic changes at the Hawaii Ocean Time Series station. *J Phys Oceanogr* 38:1931–1948.
23. Karl DM, *et al.* (1996) Seasonal and interannual variability in primary production and particle flux at Station ALOHA. *Deep-Sea Res II* 43:539–568.
24. Buesseler KO, et al. (2008) VERTIGO (VERtical Transport In the Global Ocean): A study of particle sources and flux attenuation in the North Pacific. *Deep-Sea Res II* 55:1522–1539.
25. Sheridan CC, Landry MR (2004) A 9-year increasing trend in mesozooplankton biomass at the Hawaii Ocean Time-series Station ALOHA. *ICES J Mar Sci* 61:457–463.
26. Hannides CCS, *et al.* (2009) Export stoichiometry and migrant-mediated flux of phosphorus in the North Pacific subtropical gyre. *Deep-Sea Res I* 56:73–88.
27. Corno G, *et al.* (2007) Impact of climate forcing on ecosystem processes in the North Pacific subtropical gyre. *J Geophys Res* 10.1029/2006JC003730.
28. Sabine CL, Feely RA, Watanabe YW, Lamb M (2004) Temporal evolution of the North Pacific CO_2 uptake rate. *J Oceanogr* 60:5–15.
29. Zhang J-Z, Fischer CJ, Ortner PB (1999) Laboratory glassware as a contaminant in silicate analysis of natural water samples. *Wat Res* 33:2879–2883.
30. Dickson AG (2001) Reference materials for oceanic CO_2 measurements. *Oceanography* 14:21–22.
31. McNeil BI, Matear RJ (2008) Southern Ocean acidification: A tipping point at 450-ppm atmospheric CO_2. *Proc Natl Acad Sci USA* 105:18860–18864.
32. Karl DM, Letelier RM (2008) Nitrogen fixation-enhanced carbon sequestration in low nitrate, low chlorophyll seascapes. *Mar Ecol Prog Ser* 364:257–268.
33. Dore JE, Letelier RM, Church MJ, Lukas R, Karl DM (2008) Summer phytoplankton blooms in the oligotrophic North Pacific subtropical gyre: Historical perspective and recent observations. *Prog Oceanogr* 76:2–38.